NMR evidence for common superconducting and pseudogap phase diagrams of $YBa_2Cu_3O_{7-\delta}$ and $La_{2-x}Sr_xCaCu_2O_6$

G. V. M. Williams and J. L. Tallon
New Zealand Institute for Industrial Research and Development, P.O. Box 31310, Lower Hutt, New Zealand

R. Michalak and R. Dupree
Department of Physics, University of Warwick, Coventry CV4 7AL, United Kingdom

(Received 30 April 1996)

We report ac susceptibility and ^{17}O nuclear-magnetic-resonance (NMR) measurements on the double-CuO_2-layer $La_{2-x}Sr_xCaCu_2O_6$ high-temperature superconducting cuprate (HTSC) with a $T_{c,\max}$ of 60 K. A comparison is made with ^{89}Y NMR measurements on $YBa_2Cu_3O_{7-\delta}$, which has a higher $T_{c,\max}$ of 93 K and $Y_{0.8}Ca_{0.2}Ba_2Cu_3O_{7-\delta}$ with a slightly lower $T_{c,\max}$ of 87 K. We find that the hole concentration dependence of the normal-state gap and of T_c both scale with $T_{c,\max}$, implying a universal scaled phase diagram for these two superconductors, and, by implication, for the wider class of HTSC. This suggests that the normal-state gap and the pairing mechanism may have a common origin. [S0163-1829(96)51434-7]

A variety of theories exist to explain superconductivity and the pairing mechanism in high-temperature superconducting cuprates,[1–5] but there is no clear consensus as to which theory is appropriate. Recent SQUID[6] and Raman[7] measurements have shown strong evidence for *d*-wave superconductivity. Any theory will need to explain the origin of the gap, described here as the normal-state gap, observed in NMR,[8] specific heat,[9] susceptibility,[10] resistivity,[11] and thermopower[12] measurements, that is strongly correlated with hole concentration, decreasing to zero at a hole concentration of about $p=0.19$. Recent specific heat and susceptibility measurements by Loram *et al.*[13] have shown that the normal-state gap can be described conveniently by a gap in the total density of states (DOS), where both the specific heat and susceptibility data can be modeled by a weakly interacting Fermi liquid approach. In the underdoped region the correlations associated with the normal-state gap clearly compete with superconductivity and account for the shape of the phase curve $T_c(p)$ in that region.[14] In the presence of the normal-state gap both T_c and the condensation energy are strongly depressed because of the decrease in the number of states available to create pairs.[15] In the overdoped region there is evidence that excitations above the normal-state gap may be responsible for pair breaking, which again depress T_c and the superfluid density.[14] The p dependence of E_g thus appears to be linked closely to the overall p dependence of T_c.[4]

The dependence of T_c on hole concentration follows a universal scaled function approximated by $T_c=T_{c,\max}[1-82.6(p-0.16)^2]$ indicating an underlying mechanism, which is common to all superconducting cuprates[16] and for which the only variation, which occurs amongst the different cuprates appears to lie in the energy scale of the superconducting gap. It is, therefore, important that the normal-state gap be investigated in superconductors with different maximum T_c values to ascertain if the normal-state gap also is a universal scaled function of p.

In this paper we report ^{17}O NMR measurements on $La_{2-x}Sr_xCaCu_2O_6$ with a $T_{c,\max}$ of 60 K and compare them with ^{89}Y NMR measurements on $Y_{0.8}Ca_{0.2}Ba_2Cu_3O_{7-\delta}$ with a $T_{c,\max}$ of 87 K, $YBa_2Cu_4O_8$, $YBa_2Cu_3O_{7-\delta}$ with a $T_{c,\max}$ of 93 K, and $Y_2Ba_4Cu_7O_{15-\delta}$ with a $T_{c,\max}$ of 95 K. Each of these superconducting cuprates has two superconducting CuO_2 planes per repeat unit and hence effects that may be attributed to a different number of CuO_2 planes are absent. For example, NMR spectra for $YBa_2Cu_3O_{7-\delta}$ and $La_{2-x}Sr_xCuO_4$ have been interpreted in terms of antiferromagnetic interplanar coupling for $YBa_2Cu_3O_{7-\delta}$ and SDW ordering prevented by low spatial dimensionality for $La_{2-x}Sr_xCuO_4$ (Ref. 17). The $La_{2-x}Sr_xCaCu_2O_6$, $YBa_2Cu_4O_8$, $YBa_2Cu_3O_{7-\delta}$, $Y_{0.8}Ca_{0.2}Ba_2Cu_3O_{7-\delta}$, and $Y_2Ba_4Cu_7O_{15-\delta}$ superconductors have the advantage that good quality samples can be produced on the underdoped side. Most single CuO_2 layer samples have the disadvantage in that oxygen defects are known to occur on the CuO_2 plane[18] leading to broad NMR resonances.[19] Also for the single CuO_2 layer $La_{2-x}Sr_xCuO_4$ superconductor, a structural phase transition occurs at an underdoped hole concentration of $p=0.125$ (Ref. 20) and phase separation can occur in overdoped samples.[21] Other single CuO_2 layered samples are difficult to underdope and underdoping invariably leads to broad superconducting transitions. For the $Bi_2Sr_2Ca_{n-1}Cu_nO_{4+2n}$ superconductors, an incommensurate structural modulation is known to occur,[22] while cation disorder is present in the $Tl_2Ba_2Ca_{n-1}Cu_nO_{4+2n}$ and $TlBa_2Ca_{n-1}Cu_nO_{3+2n}$ superconductors.[23] Triple CuO_2 layered superconductors have the disadvantage that the outer CuO_2 layers have a different hole concentration from the inner CuO_2 layer.[24,25] We will show that the data for the double layer compounds investigated here are consistent with a p dependence of the normal-state gap that scales with $T_{c,\max}$ implying a universal phase diagram for these compounds.

$La_{2-x}Sr_xCaCu_2O_6$ ceramic samples with $x=0.08$, 0.12, 0.16, and 0.22 were prepared by decomposing in a gold crucible a stoichiometric mix of La_2O_3, $Sr(NO_3)_2$, $Ca(NO_3)_2$, and CuO powders for 1 h in air at 700 °C. The samples were

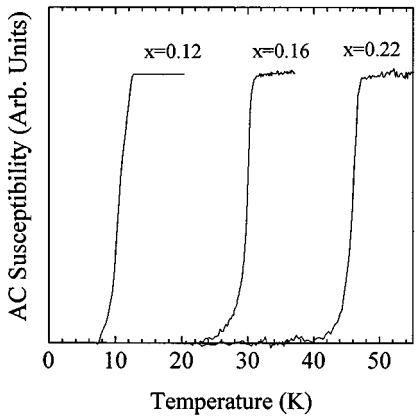

FIG. 1. Plot of ac susceptibility against temperature for $La_{2-x}Sr_xCaCu_2O_6$ superconductors with Sr fractions indicated.

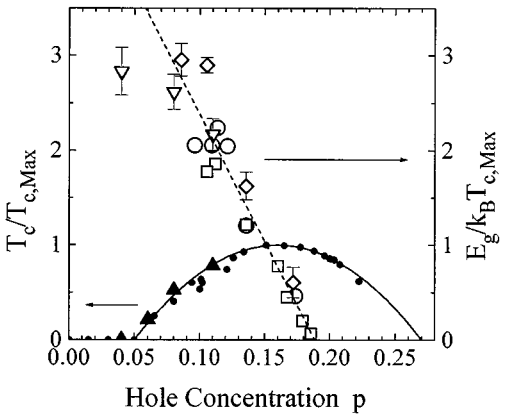

FIG. 2. Plot of $T_c/T_{c,\max}$ against hole concentration for $Y_{1-x}Ca_xBa_2Cu_3O_6$, $YBa_2Cu_3O_{7-\delta}$, $Y_{1-x}Ca_xBa_2Cu_3O_7$ (filled circles) (Ref. 30), and $La_{2-x}Sr_xCaCu_2O_6$ (filled up triangles). The solid curve is $T_c/T_{c,\max} = [1-82.6(p-0.16)^2]$ (Ref. 18). Also included is $E_g/k_BT_{c,\max}$ plotted against hole concentration for $YBa_2Cu_3O_{7-\delta}$, $YBa_2Cu_4O_8$, and $Y_2Ba_4Cu_7O_{15-\delta}$ determined from ^{89}Y NMR data (open circles) (Refs. 12,33), $YBa_2Cu_3O_{7-\delta}$ as determined from specific heat measurements (open squares) (Ref. 12), $Y_{0.8}Ca_{0.2}Ba_2Cu_3O_{7-\delta}$ determined from ^{89}Y NMR data (open diamonds), and the $La_{2-x}Sr_xCaCu_2O_6$ determined from ^{17}O NMR data (open down triangles). The dashed line is a guide to the eye.

initially reacted for 24 h at 925 °C in O_2 at a pressure of 1 bar. This was followed by further reactions at an O_2 pressure of 60 bar and temperatures of 900, 1010, 1030, and 1050 °C for 48 h. The samples were reground after each reaction. The final reaction was followed by a 72 h anneal at 350 °C in an O_2 pressure of 60 bar in order to, as much as possible, eliminate oxygen vacancies. Under these conditions, it was not possible to produce samples with $x>0.22$ for which higher oxygen partial pressures are required.[26] XRD analysis indicated that the samples were single phase.

$Y_{0.8}Ca_{0.2}Ba_2Cu_3O_{7-\delta}$ samples were prepared by initially decomposing a stoichiometric mix of Y_2O_3, $Ca(NO_3)_2$, $Ba(NO_3)_2$, and CuO powders in a gold crucible at 700 °C in air. This was followed by further reactions in air at 900 °C for 6 h, and 915, 930, 940, and 950 °C for 24 h. The samples were reground after each reaction. The samples were annealed in nitrogen-oxygen gases at a variety of oxygen partial pressures and temperatures to achieve a range of T_c values. XRD analysis showed that the samples were single phase. There was no evidence of the $Ba_4CaCu_3O_8$ and $BaCuO_2$ defect phases, which are known to occur when there is partial Ca substitution for Ba instead of Y.

The $La_{2-x}Sr_xCaCu_2O_6$ samples were ^{17}O exchanged by annealing in 10% ^{17}O enriched O_2. The annealing temperatures were 700 °C for 10 h followed by 350 °C for 24 h. The ^{17}O NMR spectra were measured between 10 K and room temperature using a Bruker MSL 360 spectrometer and a 8.45 T superconducting magnet. The 90°-τ-180° spin-echo technique was used to acquire the ^{17}O NMR data with delays of 100 ms to 4 s. The spectra were referenced to H_2O. Variable temperature magic angle spinning ^{89}Y NMR measurements were made on the $Y_{0.8}Ca_{0.2}Ba_2Cu_3O_{7-\delta}$ samples in the temperature range 110–300 K using a Varian Unity 500 spectrometer with a 11.74 T superconducting magnet. Samples were spun at a frequency of $\sim$2.5 kHz to reduce the linewidth and the spectra were acquired using the spin-echo technique with τ set to one rotor period. The NMR shifts were referenced to a 1 m aqueous solution of YCl_3. ac susceptibility measurements were made between 4 K and room temperature.

The $La_{2-x}Sr_xCaCu_2O_6$ ac susceptibility data are presented in Fig. 1 for $x=0.12$, 0.16, and 0.22 with corresponding T_c values of 12.7, 31.5, and 47 K, respectively. The $x=0.08$ sample is not superconducting. The quality of the samples can be seen by the narrow superconducting transitions widths, $T_c(\text{onset})-T_c(\text{mid}) = 2.2$, 1.6, and 1.2 K, respectively, for the $x=0.12$, 0.16, and 0.22 samples. By comparison, superconducting transition widths of 12–20 K are often reported for this superconductor.[26,27] We show in Fig. 2, where $T_c/T_{c,\max}$ is plotted against $p=x/2$, that the universal scaling relation approximated by $T_c/T_{c,\max} = [1-82.6(p-0.16)^2]$ is also valid for this superconductor.[16] Also included in Fig. 2 is $T_c/T_{c,\max}$ for $YBa_2Cu_3O_{7-\delta}$ and $Y_{1-x}Ca_xBa_2Cu_3O_6$ (Ref. 28). In the case of $Y_{1-x}Ca_xBa_2Cu_3O_6$ (i.e., with $\delta = 1$) the values $T_c/T_{c,\max}$ are plotted against $x/2$ indicating that each Ca contributed 0.5 holes per CuO_2 plane.

Typical room-temperature $La_{2-x}Sr_xCaCu_2O_6$ ^{17}O NMR spectra are presented in Fig. 3 for $x=0.08$, where the delay was 4 s [Fig. 3(a)] or 50 ms [Fig. 3(b)]. We show that the spectra can be modeled by three Gaussians centered on 437, 1126, and 1123 ppm and labeled 1, 2, and 3, where the fitted FWHM's were 150, 330, and 1600 ppm. By comparison with previous ^{17}O measurements on $Bi_2Sr_2Ca_{n-1}Cu_nO_{4+2n}$ (Ref. 29) and $Tl_2Ba_2Ca_{n-1}Cu_nO_{4+2n}$ (Ref. 25) we attribute peak 1 to oxygen atoms that are in an insulating environment and not in the CuO_2 plane. This is consistent with peak 1 having a long spin-lattice relation time, where this peak is nearly eliminated for the short delay of 50 ms. We attribute peak 2, with a FWHM of 330 ppm to oxygen atoms in the CuO_2 plane. Peak 3 is very broad with a FWHM of 1600 ppm, and we attribute it to regions of cation disorder. Similar broad peaks observed in $La_{2-x}Sr_xCuO_4$ and $Tl_2Ba_2CuO_4$ have been attributed to oxygen and cation disorder and possible oxygen vacancies on the CuO_2 planes.[19] We find that, unlike peak 2, the resonance position of the broad peak is independent of temperature. Neutron diffraction measurements on $La_{2-x}Sr_xCaCu_2O_6$ have shown that cation disor-

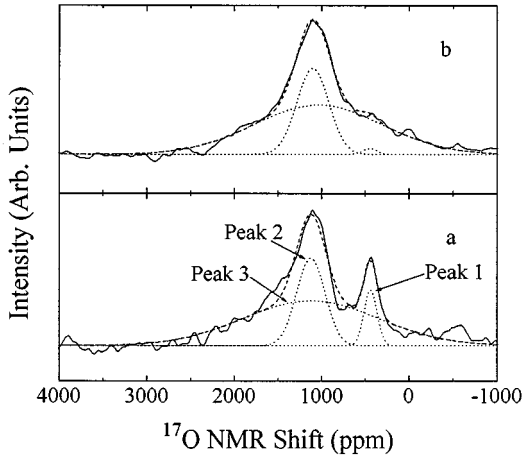

FIG. 3. Plot of the ^{17}O NMR spectra for $La_{1.92}Sr_{0.08}CaCu_2O_6$ with pulse repetition times of (a) 4 s and (b) 50 ms. The dashed curve is the best fit to the data from three separate Gaussians (dotted curves).

der in the form of intersubstitution of La and Ca is possible. Furthermore, partial occupancy (up to 7%) of an oxygen site in between the CuO_2 planes also is known to occur.[26]

The $La_{2-x}Sr_xCaCu_2O_6$ ^{17}O NMR shift is plotted in Fig. 4(a) for $x = 0.08$, 4(b) for $x = 0.16$, and 4(c) for $x = 0.22$. In the ionic model of Mila and Rice[30] the ^{17}O NMR shifts in Fig. 4 can be described by $^{17}K_{\rm iso} = 2C\chi_s + \sigma$, where C is the transferred hyperfine coupling constant from the 2 nearest Cu atoms, χ_s is the spin density of states, and σ is the chemical shift. The decrease in the NMR shift as the temperature is reduced below room temperature has been interpreted in terms of the opening of a normal-state gap.[8–12] We have shown previously that the $YBa_2Cu_3O_{7-\delta}$, $Y_2Ba_4Cu_7O_{15-\delta}$, and $YBa_2Cu_4O_8$ ^{89}Y NMR shifts can be

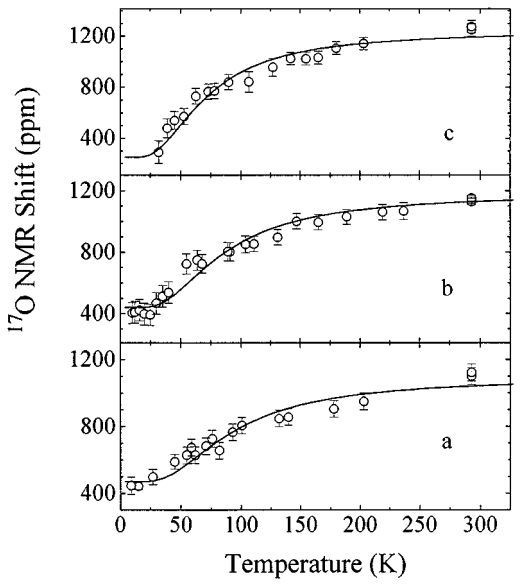

FIG. 4. Plot of the $La_{2-x}Sr_xCaCu_2O_6$ ^{17}O NMR shift (a) $x = 0.08$, (b) $x = 0.16$, and (c) $x = 0.22$. The curves are the best fit to the data using Eq. (1) in the text.

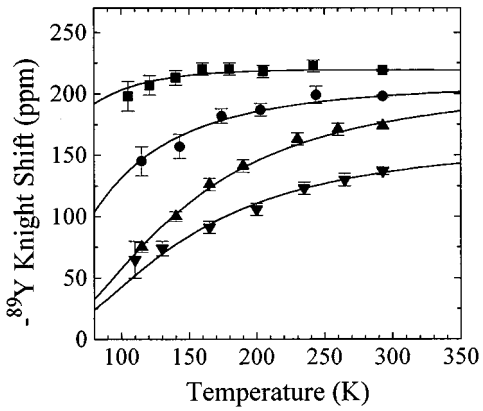

FIG. 5. Plot of the ^{89}Y NMR Knight shift for $Y_{0.8}Ca_{0.2}Ba_2Cu_3O_{7-\delta}$, where T_c is 47.5 K (filled down triangles), 65.8 K (filled up triangles), 83.2 K (filled circles), and 86 K (filled squares). The curves are the best fits to Eq. (1) in the text.

modeled by a step function gap in the DOS, which fills in with increasing temperature, leading to a NMR shift of the form,

$$K = K_0 \mathrm{sech}^2(E_g/2k_BT) + K_1 + \sigma, \qquad (1)$$

where E_g is the normal-state gap and K_1 accounts for filling in of the gap.[31,32] Thus we fit Eq. (1) to the ^{17}O NMR data in Fig. 4, where we find that $E_g/k_B = (170 \pm 15)$K, (157 ± 11)K, and (130 ± 10)K, respectively, for $x = 0.08$, 0.16, and 0.22. K_1 is 0 for $x = 0.22$, 191 ppm for $x = 0.16$, and 213 ppm for 0.08. Similar behavior observed from specific heat measurements on very underdoped $YBa_2Cu_3O_{7-\delta}$ (Ref. 9) has been interpreted in terms of filling in of the normal-state gap.

In Fig. 5 we show ^{89}Y NMR Knight shift for $Y_{0.8}Ca_{0.2}Ba_2Cu_3O_{7-\delta}$ samples with T_c values of 47.5, 65.8, 83.2, and 86.0 K. In the ionic model of Mila and Rice[30] the total ^{89}Y NMR shift is $^{89}K = 8D\chi_s + \sigma$, where D is the transferred hyperfine coupling constant from the eight nearest Cu atoms, χ_s is the spin density of states, and σ is the chemical shift (152 ppm, Ref. 32). We fit the ^{89}Y NMR Knight shift in Fig. 5 to Eq. (1) and find E_g/k_B values of (258 ± 14)K, (253 ± 7)K, (142 ± 13)K, and (53 ± 14)K for $T_c = 47.5$, 65.8, 83.2, and 86.0 K, respectively. The resultant $E_g/k_BT_{c,\max}$ values are plotted in Fig. 2 against hole concentration (open diamonds), where the hole concentration was estimated from $T_c/T_{c,\max} = [1 - 82.6(p - 0.16)^2]$. Also included in Fig. 2 are $E_g/k_BT_{c,\max}$ values determined from ^{89}Y NMR on $YBa_2Cu_3O_{7-\delta}$, $YBa_2Cu_4O_8$, and $Y_2Ba_4Cu_7O_{15-\delta}$ (open circles).[12,31] We note that thermopower and NMR measurements have shown[33] that the electronic behavior in the CuO_2 planes in $YBa_2Cu_4O_8$ is equivalent to an underdoped $YBa_2Cu_3O_{7-\delta}$ superconductor with $\delta \sim 0.2$.[34] Also shown by the open squares in Fig. 2 is $E_g/k_BT_{c,\max}$ for $YBa_2Cu_3O_{7-\delta}$ as determined from specific heat measurements.[12] For these compounds with similar $T_{c,\max}$ values, $E_g/k_BT_{c,\max}$ decreases linearly with hole concentration reaching zero at $p \sim 0.19$.

The $La_{2-x}Sr_xCaCu_2O_6$ normal-state gap is compared with that of the $YBa_2Cu_3O_{7-\delta}$ family of superconductors in

Fig. 2, where we plot $E_g/k_BT_{c,\max}$ determined from the ^{17}O NMR measurements. It can be seen that values of $E_g/k_BT_{c,\max}$ for both the $YBa_2Cu_3O_{7-\delta}$ family and $La_{2-x}Sr_xCaCu_2O_6$ follow the same line implying not only a universal scaled phase diagram for T_c, but also for the normal-state pseudogap.

Recent heat capacity,[13] susceptibility,[13] and ARPES[35] evidence that the normal-state pseudogap has the same (possibility d-wave) anisotropy as does the superconducting gap gives strong credence to models in which these gaps are intimately related. These results together with the present data would appear to support strongly the model of Emery and Kivelson[36] in which the pseudogap is associated with short-range pairing correlations, while the lower superconducting transition temperature is associated with long-range phase coherence.

In conclusion, we find that not only does $T_c(p)$ scale with $T_{c,\max}$ on the same p-dependent phase curve, but that the normal-state gap $E_g(p)$ observed in the ^{17}O and ^{89}Y Knight shift data also scales with $T_{c,\max}$ for the $YBa_2Cu_3O_{7-\delta}$ family and $La_{2-x}Sr_xCaCu_2O_6$ superconductors. The occurrence of a common scaled phase diagram for these two parameters suggests that the normal state gap originates from the same mechanism that is responsible for the superconducting pairing and lends strong evidence to the model of Loram *et al.*[14] in which the depression in T_c and pair density with underdoping is because of the opening of the normal-state gap. Within this model, common scaling behavior in $T_c(p)$ demands common scaling behavior in $E_g(p)$.

This work was supported by EPSRC. GVMW acknowledges travel assistance from the New Zealand MORST ISAC Programme, Grant No. 94/29.

[1] A. J. Millis, H. Monien, and D. Pines, Phys. Rev. B **142**, 167 (1990).
[2] A. I. Liechtenstein, I. I. Mazin, and O. K. Andersen, Phys. Rev. Lett. **74**, 2303 (1995).
[3] N. F. Mott, Adv. Phys. **39**, 55 (1990).
[4] C. M. Varma *et al.*, Phys. Rev. Lett. **63**, 1996 (1989).
[5] M. L. Kulic *et al.*, Physica C **244**, 184 (1995).
[6] J. R. Kirtley *et al.*, Nature **373**, 225 (1995).
[7] X. K. Chen *et al.*, Phys. Rev. Lett. **73**, 3290 (1994).
[8] J. Alloul *et al.*, Phys. Rev. Lett. **71**, 1740 (1993).
[9] J. Loram *et al.*, Phys. Rev. Lett. **71**, 1740 (1993).
[10] D. C. Johnston, Phys. Rev. Lett. **62**, 957 (1989).
[11] B. Bucher *et al.*, Phys. Rev. Lett. **70**, 2012 (1993); I. Ito, K. Takenaka, and S. Uchida, *ibid.* **70**, 3995 (1993).
[12] J. L. Tallon *et al.*, Phys. Rev. Lett. **75**, 4414 (1995).
[13] J. W. Loram, J. R. Cooper, K. A. Mizra, N. Athanassopoulou, and W. Y. Liang (unpublished).
[14] J. L. Tallon *et al.*, Physica C **235-240**, 1821 (1994).
[15] J. W. Loram *et al.*, J. Supercond. **7**, 243 (1994).
[16] M. R. Presland *et al.*, Physica C **165**, 391 (1991).
[17] A. J. Millis and H. Monien, Phys. Rev. Lett. **70**, 2810 (1993).
[18] J. B. Torrance *et al.*, Phys. Rev. Lett. **61**, 1127 (1988).
[19] E. Oldfield *et al.*, Phys. Rev. B **40**, 6832 (1989).
[20] P. G. Radaelli *et al.*, Phys. Rev. B **49**, 4163 (1994).
[21] J. D. Jorgensen, in *Advances in Superconductivity III*, edited by K. Kajimura and H. Hagakawa (Springer-Verlag, Tokyo, 1991), p. 337.
[22] J. L. Tallon *et al.*, Nature **333**, 153 (1988).
[23] M. A. G. Aranda, D. C. Sinclair, and J. P. Attfield, Physica C **221**, 304 (1994).
[24] E. M. Haines and J. L. Tallon, Phys. Rev. B **45**, 3172 (1992).
[25] A. P. Howes *et al.*, Phys. Rev. B **47**, 11 529 (1993).
[26] G. H. Kwei *et al.*, Physica C **213**, 455 (1993).
[27] C.-J. Liu and H. Yamauchi, Phys. Rev. B **51**, 11 826 (1995).
[28] J. L. Tallon *et al.*, Phys. Rev. B **51**, 12 911 (1995).
[29] R. Dupree *et al.*, Physica C **175**, 269 (1991).
[30] F. Mila and T. M. Rice, Physica C **157**, 571 (1989).
[31] G. V. M. Williams *et al.*, Phys. Rev. B **51**, 16 503 (1995).
[32] G. V. M. Williams *et al.*, Physica C **258**, 273 (1996).
[33] M. Takigawa, W. L. Hults, and J. L. Smith, Phys. Rev. Lett. **71**, 2650 (1993).
[34] R. Dupree *et al.*, Physica C **179**, 311 (1991).
[35] A. G. Loeser *et al.*,Science **283**, 325 (1996).
[36] V. J. Emery and S. A. Kivelson, Nature **374**, 434 (1995).